ARTICLE

Reversibility, Dopant Desorption, and Tunneling in the Temperature-Dependent Conductivity of Type-Separated, Conductive Carbon Nanotube Networks

Teresa M. Barnes,* Jeffrey L. Blackburn, Jao van de Lagemaat, Timothy J. Coutts, and Michael J. Heben

National Renewable Energy Laboratory, Golden, Colorado 80401

ABSTRACT We present a comprehensive study of the effects of doping and temperature on the conductivity of single-walled carbon nanotube (SWNT) networks. We investigated nearly type-pure networks as well as networks comprising precisely tuned mixtures of metallic and semiconducting tubes. Networks were studied in their as-produced state and after treatments with nitric acid, thionyl chloride, and hydrazine to explore the effects of both intentional and adventitious doping. For intentionally and adventitiously doped networks, the sheet resistance (R_s) exhibits an irreversible increase with temperature above ~350 K. Dopant desorption is shown to be the main cause of this increase and the observed hysteresis in the temperature-dependent resistivity. Both thermal and chemical dedoping produced networks free of hysteresis. Temperature-programmed desorption data showed that dopants are most strongly bound to the metallic tubes and that networks consisting of metallic tubes exhibit the best thermal stability. At temperatures below the dopant desorption threshold, conductivity in the networks is primarily controlled by thermally assisted tunneling through barriers at the intertube or interbundle junctions.

KEYWORDS: carbon nanotubes · doping · hysteresis · optical properties · electrical properties · resistivity · temperature dependence

In contrast to thick "bucky papers",[1−3] thin mats of entangled carbon single-walled nanotubes (SWNTs) can be simultaneously highly transparent and electrically conducting. Consequently, thin SWNT films are being investigated for use in a variety of technologies such as photovoltaics, flat-panel displays, and others applications that currently rely upon transparent conducting oxides (TCOs) such as In_2O_3:Sn, ZnO:Al, or SnO_2:F.[4] In addition to the potential for low cost due to the abundance of carbon, thin SWNT films offer several important benefits over traditional TCOs. In particular, thin SWNT mats are preferentially hole-conducting, highly amenable to low-temperature solution deposition, and inherently flexible.[5−7] To date, however, SWNT films have not yet matched the optoelectronic performance and thermal stability found in high-quality TCO materials.

Many factors affect the conductivity of SWNT networks, including tube length and diameter,[8] chemical doping,[9] and network morphology.[1,10] Individual tubes show clear metallic or semiconducting behavior depending on chirality and band structure,[11] so tube type should also affect network conductivity.[12] However, the transport behavior of thin SWNT mats is complicated because as-synthesized materials are typically a mixture of ~1/3 metallic m-SWNTs and ~2/3 semiconducting s-SWNTs. Thin-film networks formed from as-synthesized SWNT distributions show a negative temperature dependence of resistance ($dR/dT < 0$) at low temperatures and a change to a positive dependence ($dR/dT > 0$) above a transition temperature (T^*). This so-called U-shaped temperature dependence of resistivity has been widely reported[13,14] and has been ascribed to a transition from semiconducting to metallic transport behavior. Several groups have proposed that the transport is limited by Schottky barriers between s- and m-SWNTs at low T,[1,15,16] while at higher T, the conductivity is thought to be controlled by percolation pathways between m-SWNTs.[1] This view implies that a network of pure m-SWNTs would have higher conductivity at low T than either films formed from pure s-SWNTs or films formed from mixtures of s- and m-SWNTs and a positive temperature coefficient of resistivity. However, recent observations demonstrate that electrical transport in thin SWNT films is dominated by tube−tube junctions and doping effects for both m-

*Address correspondence to teresa_barnes@nrel.gov.

Received for review March 26, 2008 and accepted August 21, 2008.

Published online September 23, 2008.
10.1021/nn800194u CCC: $40.75

and s-SWNT-enriched networks.[17,18] Clearly, many aspects of the electrical transport mechanisms in thin SWNT films are not completely understood.

Here, we explore the temperature dependence of the resistivity in thin SWNT films from a different perspective. Utilizing materials generated in-house by laser vaporization,[17,19] and recently developed techniques for separating m- and s-SWNTs,[20,21] we prepared thin SWNT films with a variety of precisely controlled m/s-SWNT ratios.[17] A variety of chemical treatments were employed to dope and dedope the films, and the temperature-dependent transport behavior was investigated in vacuum with the four-point van der Pauw method. Surprisingly, we found that the transition to $dR/dT > 0$ behavior, which is typically assigned to the onset of metallic conductivity, is independent of the concentration of m-SWNTs in these films. Furthermore, the magnitude of the $dR/dT > 0$ response was smaller when the concentration of m-SWNTs in the films was increased. In fact, the transition to $dR/dT > 0$ was not observed up to 450 K for undoped films with either low or high m-SWNT contents. Thus, we conclude that the onset of $dR/dT > 0$ behavior in thin transparent networks is not associated with the transition to metallic conductivity as has been reported in the literature.[1,13,14,22] This conclusion is further supported by the observation of significant hysteresis in the temperature-dependent resistivity and the absence of reversibility. Instead, the behavior can be straightforwardly explained as conductivity changes associated with thermal desorption of molecular dopants, in agreement with the oxygen sensitivity seen previously for individual and roped tubes by Collins *et al.*[23] With this insight, we performed thermal desorption mass spectrometry and determined that m-SWNTs bind certain molecular dopants more strongly than do s-SWNTs. These findings advance the understanding of electrical transport in thin SWNT films.

RESULTS AND DISCUSSION

Figure 1a shows the measured sheet resistance (R_s) of an as-prepared film made by the vacuum filtration process[12] as a function of temperature from 100 to 450 K (see Methods for details on sample preparation). Despite thorough washing with copious amounts of water, it is well-known that residual nitric acid from the initial purification of the laser soot can still be present in these films (*vide infra*, and refs 12 and 24). Note that this film is representative of those that have been investigated by others[9] and may be described as being adventitiously doped by the purification process and/or ambient gases. The first heating cycle shows R_s decreasing with increasing temperature until a minimum is reached at T^*, ~350 K, at which point R_s begins to increase until a maximum is reached at the maximum temperature, 450 K. Dramatically different $R(T)$ behavior is observed when R_s is recorded as the film is cooled after being held at 450 K for 30 min. In fact, after 30 min at 450 K, R_s is ~50% higher than the value measured at the same temperature at the end of the first heating cycle. Furthermore, R_s continues to increase with decreasing temperature, and T^*, the transition temperature, is no longer observed. Clearly, there is substantial hysteresis and irreversibility between the

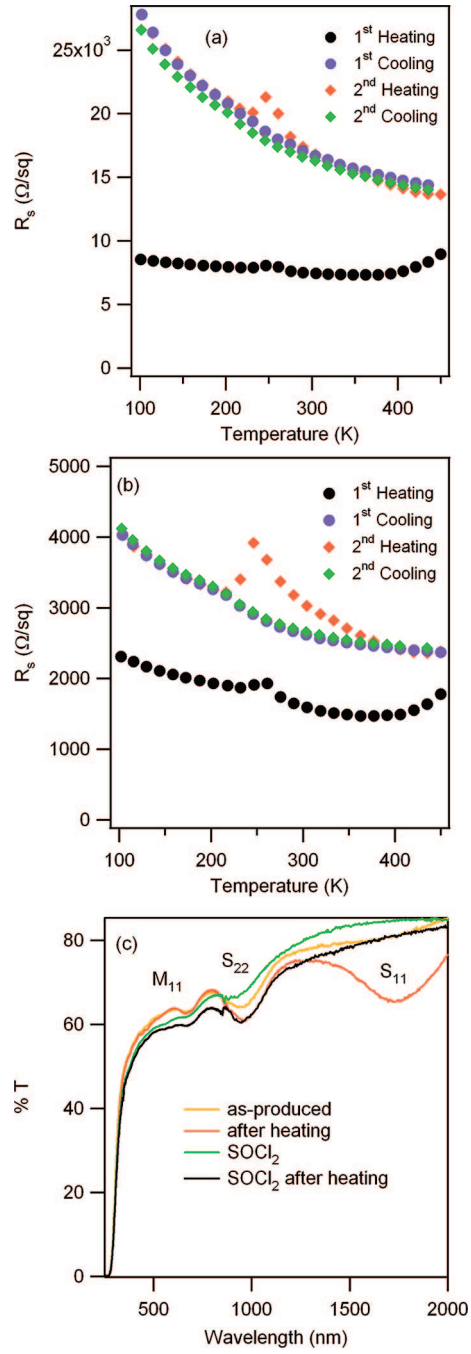

Figure 1. (a) Temperature-dependent resistivity of an "as-produced" or unintentionally doped bulk SWNT film for two heating and cooling cycles. The film was kept at 450 K for 30 min after the first heating cycle. (b) Temperature-dependent resistivity of the same film after an overnight treatment in $SOCl_2$. (c) Transmission spectra for films in (a) and (b) before and after temperature-dependent resistivity measurements.

first heating and cooling, but the second cooling and heating cycle shows no significant hysteresis and very good reversibility. Note that a hysteresis could be produced in the second cycle if the time at elevated temperatures between the first heating and cooling was reduced. Data for the same film measured after an overnight treatment in $SOCl_2$ are shown in Figure 1b. The shape of the temperature dependence is qualitatively similar for both the doped and the as-prepared films, though the absolute magnitude of the resistivity is much smaller in the former case. Also, the increase in resistivity after heating is much smaller for the $SOCl_2$-doped film. Interestingly, the second heating produces a bump in resistivity at ~250 K for both the as-prepared and $SOCl_2$-doped films. Though not fully understood at this time, this is likely due to the endothermic desorption of water species which had re-adsorbed onto the films during time spent at low T in the rough vacuum.

The data in Figure 1 may be simply understood by considering that molecular dopants, either intentionally introduced, remnant from a processing step, or present simply due to equilibration with O_2 in laboratory air, are thermally unstable and can be readily desorbed if given sufficient time and temperature to do so. Once desorbed, the changes to the electrical transport induced by the doping are also reversed. Optical transmission/absorption measurements offer a simple means by which the presence or absence of doping may be detected. Specifically, doping levels can be determined by measuring the intensities of the S_{11}, S_{22}, and M_{11} SWNT optical transitions, which may be bleached by doping.[24] Figure 1c shows transmission spectra for an unseparated film in both the as-prepared state and after treatment with $SOCl_2$, before and after heating in the temperature-dependent R_s measurement. The lowest energy S_{11} transition at ~1700 nm, which is strongly bleached by doping, is nearly absent prior to the first excursion to elevated temperature in vacuum. After heating, however, S_{11} is readily observed as the dominant absorption band in the as-prepared film. Evidently, the adventitious doping of these as-prepared films, produced by either residual nitric acid or equilibration with laboratory air, is removed as the dopant species are desorbed. In contrast, very little oscillator strength is restored to the S_{11} transition after the $SOCl_2$-doped film is heated.

The correspondence between the electrical and optical data in Figure 1a−c and the lack of a U-shaped response after the first heating excursion make it clear that the conventional description[1,14,22] of the temperature-dependent transport properties is not applicable to our findings. Clearly, a description based solely on carrier scattering processes would be fully reversible with temperature, but reversibility is not observed in our measurements except after the first heating cycle when in fact the U-shaped response is eliminated. It is important to note that we observe this behavior consistently, irrespective of film thickness, sheet resistance (50−20000 Ω/sq), or deposition technique. Consequently, it is interesting to speculate why such behavior has not been noted elsewhere in studies of electrical transport in thin SWNT films. Early resistivity measurements on thick bucky papers noted that similar changes in the shape of the $R(T)$ curve were produced by heating in vacuum, but dopant desorption and reversibility were not discussed.[3] Zhang *et al.*[25] also presented a temperature-dependent resistivity measurement up to 400 K under vacuum that shows no evidence of a transition to $dR/dT > 0$, and once again, the issue of doping was not discussed. In this case, the films were either undoped initially or the T^* value associated with dopant desorption was significantly higher than 400 K. In other studies, it must be that reversibility was always seen and considered to be unremarkable, or cycling measurements were not performed. Note that repeated measurements on a given film would yield the same U-shaped response if the temperature programs were the same and the films were permitted to equilibrate with laboratory air between measurements. Also, the reversibility we observe would not be found unless temperatures were sufficiently high to dedope the films by desorption and the atmosphere above the film was inert. Though hysteresis is well-known in the resistivity of nanotube gas sensors,[26,27] the related phenomena have not been fully appreciated by the community interested in the optoelectronic properties of thin SWNT films.

To clarify the discussion in the rest of this paper, we adopt the symbol T^*_{dedope} to signify that thermal desorption of dopants is responsible for the behavior we observe in our films, as clearly demonstrated in Figure 1a. For previous reports, we adopt the symbol $T^*_{tun\text{-}met}$ to signify that this metric defines the temperature at which the fundamental conductivity mechanism changes from **tun**neling-limited to phonon-limited (**met**allic) resistance. Our data suggest that previous studies reporting U-shaped $R(T)$ behavior with $T^*_{tun\text{-}met}$ near room temperature may have been observing artifacts from the thermal desorption of dopants, in other words, measuring T^*_{dedope}. However, we note here that we have no data to infer that reports demonstrating lower $T^*_{tun\text{-}met}$ values (*e.g.*, < 250 K) were confounded by similar artifacts.

To understand the effect of dedoping on the transport properties in more detail, we investigated the temperature dependence of R_s during the first heating using films with varying m-SWNT fractions that were not intentionally doped (Figure 2a). The SWNTs in these films were separated from unpurified bulk soots (see Methods) and were never exposed to acids, so the doping levels were only controlled by equilibration with O_2 in air. Nevertheless, the films showed the same transition to $dR/dT > 0$ behavior as films that had been exposed to acids, and similar changes in the optical prop-

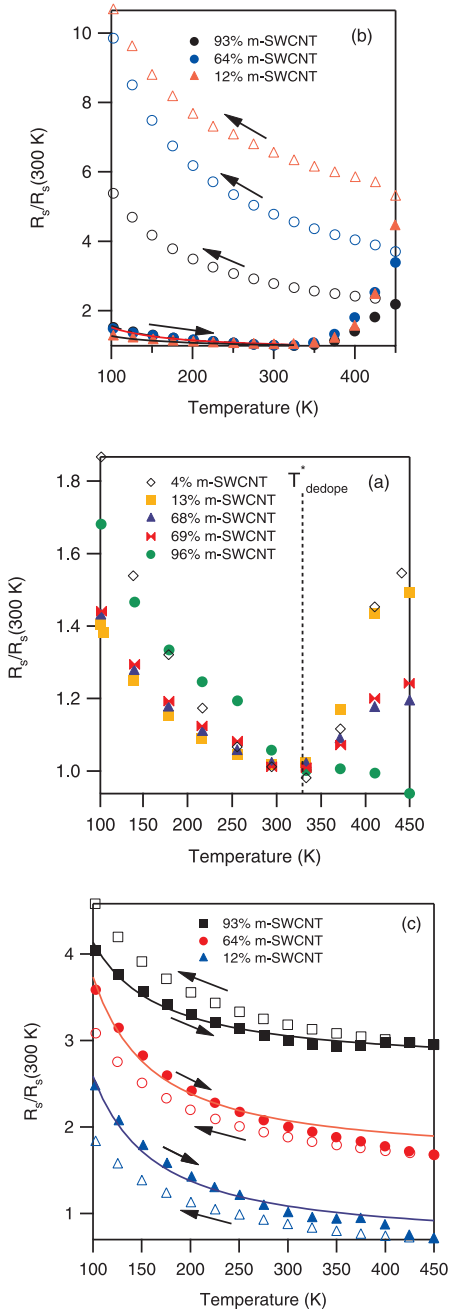

Figure 2. R_s *versus* T for films formed with various m:s-SWNT ratios: (a) first temperature scan for as-produced films that were not exposed to acids and not intentionally doped; (b) nitric acid-doped films showing hysteresis; and (c) hydrazine-treated films showing reversibility. The traces in (c) have been offset for clarity.

erties with heating. Thus, the high-temperature change in resistivity is also due to dedoping in these separated samples. Because these tubes were never exposed to acid, it is clear that adventitious doping from atmospheric impurities[23] can lead to these effects. It is particularly interesting to note that the rate at which R_s increases above T^*_{dedope} decreases as the m-SWNT fraction increases. Also, the value of T^*_{dedope} is not appreciably altered by changes in metallic tube content. Both of these observations are in conflict with the model that describes the U-shaped response as being due to a transition at T^* from semiconducting to metallic transport.

Qualitatively similar information is obtained when intentionally doped films are examined. Figure 2b shows the R_s *versus* T data for three films with different m:s ratios that were treated with nitric acid (see Methods). The data are presented in a normalized format, but note that the room temperature resistivity of the semiconductor-enriched film at T^*_{dedope} on the first scan is 135 Ω/sq, which is far lower than the measured R_s data presented in Figure 1a,b. Consistent with the data in Figure 1, all three curves show a large hysteresis that is associated with dopant desorption that begins at T^*_{dedope}. Consistent with the data for the adventitiously doped samples (Figure 2a), the magnitude of the $dR/dT > 0$ response above T^*_{dedope} is related to the s-SWNT content in the films. The degree of hysteresis found with decreasing temperature is also a strong function of the s-SWNT content since s-SWNTs are more sensitive than m-SWNTs to dopant-induced changes in carrier concentrations.[17,18]

If the increase in R_s above T^* is caused primarily by dopant desorption, as our data suggest, then a completely dedoped SWNT network should not exhibit the U-shaped response and the associated irreversibility. In this case, one would expect to observe reversible behavior such as that found after desorption of dopants (Figure 1a). To test this idea, we soaked three films having a range of m:s-SWNT contents in hydrazine. Hydrazine (N_2H_4) has been shown to dedope films[17,28] *via* the addition of excess electrons.[21] Figure 2c shows the R_s *versus* T data for the same films presented in Figure 2b after treatment in hydrazine. Each film shows very good reversibility and no evidence of an upturn in R_s. Optical transmission measurements (not shown here) demonstrate that the hydrazine-treated films undergo no change in optical density after heating to 450 K, while the nitric acid doped films showed obvious dedoping after heating.

Repeating the temperature-dependent R_s experiment on intentionally and unintentionally doped films yielded similar results to those observed in Figure 2. Many chemical doping treatments for SWNT networks exist in the literature, and we tested HNO_3[24] and $SOCl_2$[29] extensively on separated samples because these treatments yielded the highest conductivity, with $SOCl_2$ exhibiting the best thermal stability.[17] HNO_3 has been shown to chemically dope the networks by shifting the Fermi level into the valence band[24] and also improve conductivity by network densification through residual surfactant removal.[10] AFM (atomic force microscopy) does not show a significant change in thickness in our films, and there appears to be little residual surfactant in the networks. Nevertheless, HNO_3

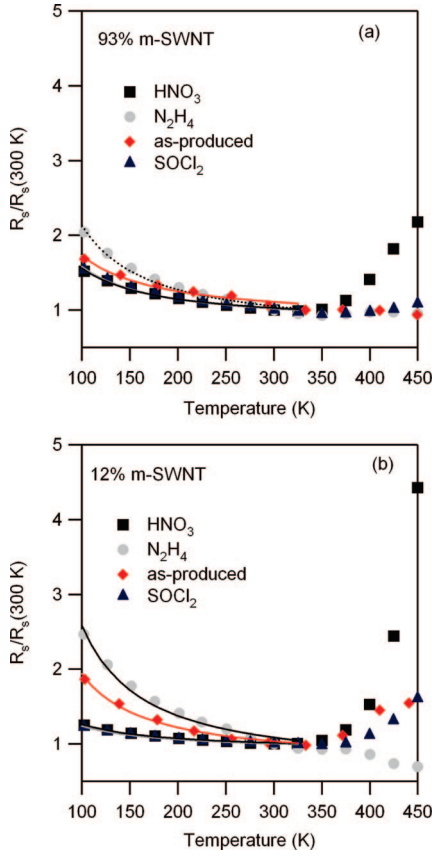

Figure 3. Normalized R_s as a function of temperature for (a) 93% metallic SWNT film and (b) 12% metallic SWNT film as-produced and after treatment in HNO_3, N_2H_4, and $SOCl_2$.

may remove trace amounts of surfactants that adversely affect conductivity.

Figure 3 shows the effects of different chemical treatments on a (a) metallic SWNT-enriched network and (b) semiconducting SWNT-enriched network. Both plots illustrate similar phenomena, but the overall change in sheet resistance is much larger for the semiconductor-enriched sample than for the metal-enriched one. The value of T^*_{dedope} is not strongly dependent on tube type and varies only from ~325 K for adventitious and HNO_3 doping to ~375 K for $SOCl_2$. At $T < T^*_{dedope}$, the slope of the R_s *versus* T curve decreases as the doping level increases from the N_2H_4-treated, to the adventitiously doped, to the HNO_3- and $SOCl_2$-treated films, the latter of which have approximately equal doping levels. The opposite is true at $T > T^*_{dedope}$. At $T > T^*_{dedope}$, R_s increases most dramatically for films treated in nitric acid and shows little or no change for the films treated in hydrazine. $SOCl_2$ appears to be much more stable than HNO_3 or adventitious doping for the semiconductor-enriched film. In general, the metal-enriched films exhibit far smaller changes in R_s with doping than the films containing significant fractions of semiconducting tubes, which is consistent with our previous findings.[17] In agreement with the results shown in Figure 2, these data suggest that conductivity in networks composed of predominantly metallic tubes should exhibit better stability with temperature than semiconducting networks. This has also been observed in a recent comparison of a metal-enriched film with an unseparated bulk sample.[30]

Electrical Transport at Low Temperatures. Below T^*_{dedope}, the temperature dependence of the resistivity is fairly weak, suggesting that a tunneling process may be controlling the conductivity at lower temperatures. Several authors have used a tunneling equation similar to eq 1 to model resistivity in SWNT networks at all measured temperatures.[14,22,31] Here, the linear term was used to represent the metal-like conductivity that was ascribed to the high-temperature $dR/dT > 0$ behavior. The second term was used to represent the tunneling contribution, which is dominant at lower temperatures. Similar data have been fit previously without using the linear metallic term.[31] Since the so-called metallic contribution is not evident unless dopant desorption occurs, we can set α equal to 0 to model our data and use only the tunneling term to fit our data.

$$R_s = \alpha T + \beta \exp\left(\frac{T_b}{T_s + T}\right) \quad (1)$$

The tunneling term in eq 1 was originally derived in the work of Sheng, where it was applied to a variety of disordered materials (including metallic fibril networks) exhibiting fluctuation-induced tunneling.[32] In eq 1, T_s can be described relatively simply as the temperature above which fluctuation effects become important. T_b is a considerably more complex function of the tunneling barrier height and shape as affected by the image force and local electric field. Smaller values of T_b are indicative of an effectively lower barrier height; β is a weak function of temperature that also accounts for the barrier shape and network properties, and it can be considered constant compared to the exponential portion of eq 1.[32]

The resistivity data were fit using eq 1 between 100 and 325 K ($T < T^*_{dedope}$) for each film described here. Fits to eq 1 are shown as solid lines in Figure 2b,c and Figure 3a,b. Fits are not shown for the remaining data in order to maintain clarity in the figures, but the data in all figures were fit satisfactorily with the model. The resistivity data were first plotted as $\ln(R_s)$ *versus* $1/T$ to independently calculate β from a linear fit. T_b and T_s were then fitted to the R_s *versus* T data using the previously determined β value to reduce uncertainty in the model. The fitting parameters are presented in Table 1 for several of the films after different chemical treatments. The validity of the model is demonstrated by the fact that data above 325 K for the dedoped networks treated with N_2H_4 could be represented by extrapolation of the low-temperature data. The values of T_b and T_s are consistent with literature values, but they both (T_s, in particular) have significant uncertainties.[14,32]

TABLE 1. Tunneling Parameters for Films Presented in Figures 2 and 3[a]

sample ID	T_b	T_s
metal - N_2H_4	130.64 ± 7.42	16.72 ± 8.08
mix - N_2H_4	181.62 ± 10.7	20.96 ± 8.41
semi - N_2H_4	167.68 ± 10.3	20.50 ± 8.78
metal - HNO_3	71.361 ± 3.53	10.02 ± 6.9
mix - HNO_3	66.519 ± 4.11	11.69 ± 8.75
semi - HNO_3	35.786 ± 1.43	5.05 ± 5.48
metal - $SOCl_2$	77.051 ± 3.92	11.84 ± 7.22
mix - $SOCl_2$	52.905 ± 2.05	7.65 ± 5.41
semi - $SOCl_2$	33.715 ± 0.898	4.79 ± 3.68

[a]The metallic tube contents for each sample are: metal = 93%, mix = 64%, semi = 12%. The values of T_b and T_s are mean values in a distribution due to the widely varying junction properties in the networks. The given standard deviations are indicative of the width of the distribution of values for each sample.

Large uncertainties in the fit are expected due to polydispersity in the type and number of junctions in the films. A small amount of residual surfactant in the networks may also contribute to the uncertainty in these values. All of the measured temperatures in this study are significantly above T_s in Table 1, indicating that the fluctuation effects should significantly reduce the effective barrier heights seen by the charge carriers in all samples.

This type of model was initially used to explain how a network of metallic fibers could exhibit "nonmetallic" resistivity characteristics because of the high tunneling resistance between fibers.[32] This is similar to what is observed here. In Sheng's work, $T^*_{tun\text{-}met}$ is identified to be the temperature where the tunneling resistance between bundles or tubes equals the intrinsic metallic resistance of the individual tube networks where doping is not a factor.[32] Here, the observed resistivity minimum observed during the first heating is due to the combination of tunneling resistance and dopant desorption effects. Figure 2c does not show a clear transition temperature, which indicates that the point where the tunneling resistance equals the intrinsic resistance of the bundles is greater than 450 K in a truly undoped network. This effect is masked in the doped networks, but it suggests that the tunneling resistance will dominate the resistivity in all networks at the temperatures of interest here. It is possible that $T^*_{tun\text{-}met}$ could be observed at higher temperatures, but it has not been observed in dedoped or vacuum-treated films at temperatures up to 600 K in the literature.[3,25] Although it is difficult to quantify absolute differences between the calculated values of T_s and T_b due to the wide variations in the networks, it is possible to discern some important trends. First, the values for T_b in doped networks are significantly lower than the values for N_2H_4-treated networks regardless of tube type. This suggests that doping alters the shape and/or height of the tunneling barriers in a manner that increases the tunneling probability. Also, the N_2H_4-treated metal-enriched samples show lower T_b values than the dedoped mixed or semiconductor-enriched samples. This supports the notion that the barriers between metallic tubes are easier for carriers to tunnel through in the absence of chemical dopants.[33] However, the lowest effective barriers, represented by the smallest T_b, are in the doped, semiconductor-enriched networks. This is consistent with our previous work demonstrating that those networks have the lowest resistivities compared to all other networks we have produced.[17] Improved tube−tube coupling with heavy doping has also been observed to lead to higher conductivities in bucky papers.[2]

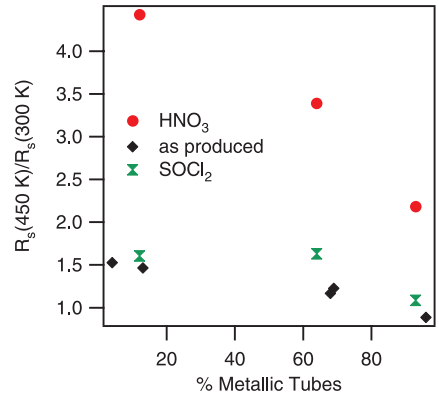

Figure 4. Ratio of R_s(450 K)/R_s(300 K) as a function of m-SWNT content for as-produced, HNO_3, and $SOCl_2$-treated samples showing a clear trend from large changes in the high-temperature resistivity for s-SWNT samples to small changes for m-SWNT samples. Note that the absolute differences in R_s(450 K)/R_s(300 K) between different dopants may be skewed by differences in the ionization ratio of active acceptors/total impurity concentration for each dopant.

Electrical Transport at High Temperatures. As shown in Figures 1, 2, and 3, R_s shows a strong temperature dependence above T^*_{dedope} for all doped films in this study. Returning to the high-temperature data in Figure 2a, R_s shows a pronounced increase above T^*_{dedope} for the film containing 4% m-SWNTs, as well as a monotonic decrease in dR/dT as the m-SWNT content is increased. This, combined with the optical data in Figure 1c and the hysteresis shown in Figures 1a,b and 2b suggests that there is a strong correlation between dopant desorption rates and m-SWNT content in the networks.

It is interesting to consider these data at $T > T^*$ with the assumption that the resistivity changes are proportional to the changes in the concentration of the adsorbed molecular dopants (*i.e.*, O_2, H_2O, *etc.*). This view is consistent with many previous nanotube sensor studies[23,34] and the switching behavior of SWNT FETs (field effect transistors) in the presence of molecular oxygen.[11,35] Figure 4 shows the relative change in sheet resistance between 450 and 300 K (R_s(450 K)/R_s(300 K)) for films with varying m-SWNT concentrations as-produced and after doping with HNO_3 and $SOCl_2$. As mentioned previously, the semiconducting samples undergo the largest changes in R_s upon heating, and the metallic samples show the smallest changes. It is somewhat difficult to compare the abso-

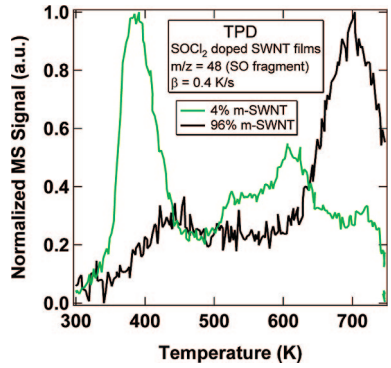

Figure 5. TPD data showing thermal desorption characteristics of $SOCl_2$. Note that the $SOCl_2$ desorbs from the semiconducting sample at around 380 K compared to at about 700 K from the metal sample.

lute differences in the R_s(450 K)/R_s(300 K) ratio for different dopants because it is highly unlikely that the total injected carrier concentration per dopant is identical for different dopants. However, the ratio of injected carriers to adsorbed dopants is probably similar for the different tube types with a single dopant. This allows the high-temperature change in resistivity to be used as a probe of molecular desorption and the change in R_s(450 K)/R_s(300 K) to be considered as representative of the relative differences in barrier heights for dopant desorption from the films. First, for all dopants, R_s(450 K)/R_s(300 K) is substantially larger for the low m-SWNT content films, indicating a low barrier to desorption. Adventitiously and HNO_3-doped films show a monotonic decrease in R_s(450 K)/R_s(300 K) with increasing m-SWNT content. $SOCl_2$-doped films show a relatively constant R_s(450 K)/R_s(300 K) for s-SWNT-enriched and mixed films and a large decrease for the heavily m-SWNT-enriched film. These data show that the dopants are most strongly bound to m-SWNTs and that mixing effects from the remaining s-SWNTs in all samples have a significant effect on dopant binding and the thermal stability of the resistivity.

Dopant desorption from the networks can be readily confirmed by temperature-programmed desorption (TPD) measurements on $SOCl_2$-treated films. Figure 5 shows that $SOCl_2$ desorbs rapidly, peaking at 400 K, from the semiconducting network, whereas the peak desorption temperature in the metal-enriched network is at almost 700 K. This is consistent with temperature-dependent resistivity measurements that show that metal-enriched films undergo less change after heating to 450 K. The TPD results demonstrate that significant amounts of dopant should desorb from the semiconductor-enriched samples at temperatures well below 450 K. The higher apparent dopant binding energies for the metal-enriched films cause the dopants to be more stable compared with the semiconductor-enriched films.

We have found two recent papers that compare relative adsorption energies of molecular dopants on s- and m-SWNTs. Yang *et al.* modeled the adsorption of NO_2 on three s-SWNTs and three m-SWNTs.[36] They found that the adsorption energy is stronger for m-SWNTs by 50−130 meV. They also suggest that the degree of charge transfer, and therefore binding energy, "will be even bigger for positively charged NO_2^+ used in real experiments." Maeda *et al.* calculated adsorption energies for methylamine (NH_2CH_3) on the (13,0) s-SWNT and (7,7) m-SWNT and found that the adsorption energy was 70−140 meV higher for the m-SWNT.[37] Our current data do not allow us to evaluate the adsorption/desorption energies with any accuracy. However, it seems clear from the data in hand that m-SWNTs have a higher affinity for dopants than do s-SWNTs, in agreement with available theory. Further experimental work on this topic is warranted.

CONCLUSIONS

We have presented data on the temperature dependence of resistivity for metallic and semiconducting SWNT-enriched transparent networks. Our data exhibit a U-shaped dependence of resistivity with temperature, but we propose a different explanation for the increase in R_s at high temperatures than is typically proposed. We show that this increase for our bulk (unseparated) and separated transparent conductive SWNT thin films may be consistently ascribed to dopant desorption. We have shown that the predominance of metallic or semiconducting SWNTs in a network does not yield the expected metallic or semiconducting dependence of resistivity on temperature but does produce important differences in electrical properties. The s-SWNT-enriched networks are extremely sensitive to chemical doping, whereas networks enriched with m-SWNTs are less affected. The temperature-dependent resistivity measurements and complementary TPD data indicate a higher dopant desorption temperature for m-SWNT-enriched networks. The data shown here suggest that the metal-like increases in R_s with temperature are due to dopant desorption, rather than truly metallic conductivity. We present a conductivity mechanism controlled by fluctuation-assisted tunneling for these networks that is able to fit the low-temperature resistivity well and is predictive of the high-temperature resistivity in chemically dedoped films. We note that other models may also fit the low-temperature-dependent behavior in these networks, but that the fluctuation-assisted tunneling model captures it well. At $T < T^*_{dedope}$, the conductivity appears to be dominated by fluctuation-assisted tunneling across tube−tube or bundle−bundle barriers. These barriers are smallest in highly doped, nearly pure semiconducting SWNT networks, likely contributing to the observed higher conductivity in these networks. These data suggest that semiconducting nanostructure net-

works may be excellent candidates for transparent conducting materials if they can be stably doped. Metallic nanostructure networks may also prove fruitful, but this work suggests that finding network materials with small tunneling barriers (low T_b values) is more important for conductivity than simply producing a network from the most highly conductive wires, rods, or tubes.

METHODS

The synthesis, purification, and separation methods used in this work are detailed elsewhere.[17] Briefly, the tubes were produced using laser vaporization (LV) of a graphite target in a nitrogen atmosphere. LV-generated soots were used to produce both bulk (unseparated) and type-separated SWNT networks. Bulk films were produced by first purifying the soot with a 16 h reflux in 3 M nitric acid. Following the reflux, the purified SWNTs were filtered through a PTFE filter membrane to create a "bucky paper." This paper was washed with successive iterations of deionized water, acetone, and 1 M KOH to remove non-nanotube carbon. Following this purification, the purified paper was dispersed by sonication in 1% sodium dodecyl sulfate (SDS) in water.

To produce type-separated films, the raw laser soot was sonicated in a cosurfactant solution and density gradient medium to separate the tubes by electronic structure.[20] We have used this method to produce SWNT solutions with metallic fractions up to 99% type-pure and semiconducting fractions as high as 95% type-pure as determined by optical absorbance spectroscopy.[17] The type-pure solutions were then mixed in varying fractions to create solutions with tuned m:s ratios. Films were deposited from these solutions by a simple vacuum filtration process.[12,17]The metallic nanotube content for each film was determined using optical absorbance spectroscopy by integrating the area underneath the second envelope of semiconducting optical transitions (S_{22}) and first envelope of metallic optical transitions (M_{11}) in the spectrum. Then the relative oscillator strengths of these transition envelopes, determined previously for our LV-SWNTs,[17] was used to calculate the relative percentages of metallic and semiconducting SWNTs. This procedure is described in more detail in ref 17.

SWNT films were doped by immersion in neat $SOCl_2$[29] or a 4 M solution of HNO_3[24] to increase their conductivity. SWNT films were dedoped by soaking in a 1 M solution of hydrazine[17,28] in ethanol or by heating the films in vacuum at 450 K for 30 min. Both dedoping treatments produced similar absorbance spectra and temperature-dependent resistance behavior. Temperature-dependent resistance measurements were obtained on an Accent Optical Hall measurement system equipped with a liquid nitrogen cryostat and a heater. Resistance measurements were conducted between 100 and 450 K in vacuum. First, the sample chamber was evacuated to a base pressure of ~0.5 Torr. Then, each sample was cooled to 100 K, where the first R_s measurement was taken. Measurements were then taken at constant temperature approximately every 15 K until the sample reached 450 K. For the sample shown in Figure 1, the temperature was fixed at 450 K for 30 min after the first heating ramp, and then measurements were taken at constant temperature every 15 K while cooling to 100 K (first cooling ramp) and immediately repeating the heating/cooling cycle (without the 30 min bake at 450 K). All other R_s measurements in this study were conducted using the same procedure without the 30 min bake at 450 K. Optical transmission before and after heating the films was obtained using a Cary 5 UV−vis−NIR spectrophotometer.

Temperature-programmed desorption was performed on <0.5 mg opaque mats of two separated films, one enriched with semiconducting SWNTs and one enriched with metallic SWNTs. Samples were placed in a platinum packet, and this platinum packet was then placed into a 2-mm-wide quartz tube. The quartz tube was affixed to the TPD apparatus *via* a VCR fitting. The sample was then pumped down *via* turbo pump to a base pressure of 7×10^{-8} Torr. It is critical to pump both separate samples (m-SWNT and s-SWNT) to the same pressure *and* to ensure that this base pressure is not too low. This detail arises from the fact that a large amount of $SOCl_2$ desorbs from the s-SWNT sample in the pump-down phase even when no heat is applied to the sample, while this is not the case for the m-SWNT sample. This is consistent with the relative desorption temperatures of $SOCl_2$ from each type of SWNT sample, shown in Figure 4. Thus, the low-temperature peak for the s-SWNT sample may not be captured if the base pressure is too low (*e.g.*, 1×10^{-8} Torr), masking the large difference in the primary desorption temperatures between the two samples.

Once the base pressure of 7×10^{-8} Torr is reached, the sample was heated linearly to 773 K *via* a copper jacket heater, at a heating rate of 0.4 K/s. The evolved chemical species were monitored with a Stanford Research Systems residual gas analyzer with a range of 1−100 amu. The full mass spectrum was recorded every 6 s. The predominant peaks were located at 32, 36, 48, 64, and 83 amu, which are consistent with the mass spectrum for thionyl chloride listed in the NIST database.[38] Kinetic traces were recorded simultaneously for these five peaks. All peaks demonstrated similar kinetic behavior, and only the peak at *m/z* of 48 (singly ionized SO) is displayed in Figure 4.

Acknowledgment. This work was supported under Department of Energy contract # DE-AC36-99GO10337. We thank the High-Efficiency Concepts Program and the U.S. DOE's Laboratory Directed Research and Development fund. We also acknowledge Robert Tenent, Jeremy Bergeson, Matt Beard, and David Young for helpful discussions.

REFERENCES AND NOTES

1. Skakalova, V.; Kaiser, A. B.; Woo, Y. S.; Roth, S. Electronic Transport in Carbon Nanotubes: From Individual Nanotubes to Thin and Thick Networks. *Phys. Rev. B* **2006**, *74*, 085403.
2. Vavro, J.; Kikkawa, J. M.; Fischer, J. E. Metal-Insulator Transition in Doped Single-Wall Carbon Nanotubes. *Phys. Rev. B* **2005**, *71*, 155410.
3. Rinzler, A.; Liu, J.; Dai, H.; Nikolaev, P.; Huffman, C. B.; Rodriguez-Macias, F. J.; Boul, P. J.; Lu, A. H.; Heymann, D.; Colbert, D. T. *et al.* Large-Scale Purification of Single-Wall Carbon Nanotubes: Process, Product, and Characterization. *Appl. Phys. A: Mater. Sci. Process.* **1998**, *67*, 29–37.
4. Gordon, R. G. Criteria for Choosing Transparent Conductors. *MRS Bull.* **2000**, *25*, 52–57.
5. Rowell, M. W.; Topinka, M. A.; McGehee, M. D.; Prall, H. J.; Dennler, G.; Sariciftci, N. S.; Hu, L. B.; Gruner, G. Organic Solar Cells with Carbon Nanotube Network Electrodes. *Appl. Phys. Lett.* **2006**, *88*, 233506.
6. Barnes, T. M.; van de Lagemaat, J.; Levi, D.; Rumbles, G.; Coutts, T. J.; Weeks, C. L.; Britz, D. A.; Levitsky, I.; Peltola, J.; Glatkowski, P. Optical Characterization of Highly Conductive Single-Wall Carbon-Nanotube Transparent Electrodes. *Phys. Rev. B* **2007**, *75*, 235410.
7. Lee, K.; Wu, Z.; Chen, Z.; Ren, F.; Pearton, S. J.; Rinzler, A. G. Single Wall Carbon Nanotubes for P-Type Ohmic Contacts to GaN Light-Emitting Diodes. *Nano Lett.* **2004**, *4*, 911–914.
8. Hecht, D. S.; Hu, L.; Gruner, G. Conductivity Scaling with Bundle Length and Diameter in Single Walled Carbon Nanotube Networks. *Appl. Phys. Lett.* **2006**, *89*, 133112.
9. Skakalova, V.; Kaiser, A. B.; Dettlaff-Weglikowska, U.; Hrncarikova, K.; Roth, S. Effect of Chemical Treatment on Electrical Conductivity, Infrared Absorption, and Raman Spectra of Single-Walled Carbon Nanotubes. *J. Phys. Chem. B* **2005**, *109*, 7174–7181.

10. Geng, H. Z.; Kim, K. K.; So, K. P.; Lee, Y. S.; Chang, Y.; Lee, Y. H. Effect of Acid Treatment on Carbon Nanotube-Based Flexible Transparent Conducting Films. *J. Am. Chem. Soc.* **2007**, *129*, 7758–7759.
11. Avouris, P. Carbon Nanotube Electronics. *Chem. Phys.* **2002**, *281*, 429–445.
12. Wu, Z.; Zhihong, C.; Xu, D.; Logan, J. M.; Sippel, J.; Nikolou, M.; Kamaras, K.; Reynolds, J. R.; Tanner, D. B.; Hebard, A. F. *et al.* Transparent, Conductive Carbon Nanotube Films. *Science* **2004**, *305*, 1273–1276.
13. Kaiser, A. B.; Park, Y. W.; Kim, G. T.; Choi, E. S.; Dusberg, G.; Roth, S. Electronic Transport in Carbon Nanotube Ropes and Mats. *Synth. Met.* **1999**, *103*, 2547–2550.
14. Shiraishi, M.; Ata, M. Conduction Mechanisms in Single-Walled Carbon Nanotubes. *Synth. Met.* **2002**, *128*, 235–239.
15. Heinze, S.; Tersoff, J.; Martel, R.; Derycke, V.; Appenzeller, J.; Avouris, P. Carbon Nanotubes as Schottky Barrier Transistors. *Phys. Rev. Lett.* **2002**, *89*, 106801.
16. Javey, A.; Guo, J.; Wang, Q.; Lundstrom, M.; Dai, H. Ballistic Carbon Nanotube Field-Effect Transistors. *Nature* **2003**, *424*, 654–657.
17. Blackburn, J. L.; Barnes, T. M.; Beard, M. C.; Kim, Y.-H.; Tenent, R. C.; McDonald, T. J.; Coutts, T. J.; To, B.; Heben, M. J. Transparent Conductive Single-Walled Carbon Nanotube Networks with Precisely Tunable Ratios of Semiconducting and Metallic Nanotubes. *ACS Nano* **2008**, *2*, 1266–1274.
18. Beard, M. C.; Blackburn, J. L.; Heben, M. J. Time-Resolved THZ Spectroscopy of Photogenerated Free-Carrier Dynamics in Metal and Semiconductor Single Walled Carbon Nanotube Films *Nano Lett.* under review.
19. Dillon, A. C.; Parilla, P. A.; Alleman, J. L.; Perkins, J. D.; Heben, M. J. Controlling Single-Wall Nanotube Diameters with Variation in Laser Pulse Power. *Chem. Phys. Lett.* **2000**, *316*, 13–18.
20. Arnold, M. S.; Green, A. A.; Hulvat, J. F.; Stupp, S. I.; Hersam, M. C. Sorting Carbon Nanotubes by Electronic Structure Using Density Differentiation. *Nat. Nanotechnol.* **2006**, *1*, 60–65.
21. Green, A. A.; Hersam, M. C. Colored Semitransparent Conductive Coatings Consisting of Monodisperse Metallic Single-Walled Carbon Nanotubes. *Nano Lett.* **2008**, *8*, 1417–1422.
22. Kaiser, A. B.; Dusberg, G.; Roth, S. Heterogeneous Model for Conduction in Carbon Nanotubes. *Phys. Rev. B* **1998**, *57*, 1418–1421.
23. Collins, P. G.; Bradley, K.; Ishigami, M.; Zettl, A. Extreme Oxygen Sensitivity of Electronic Properties of Carbon Nanotubes. *Science* **2000**, *287*, 1801–1804.
24. Zhou, W.; Vavro, J.; Nemes, N. M.; Fischer, J. E.; Borondics, F.; Kamaras, K.; Tanner, D. B. Charge Transfer and Fermi Level Shift in P-Doped Single-Walled Carbon Nanotubes. *Phys. Rev. B* **2005**, *71*, 205423.
25. Zhang, M.; Fang, S.; Zakhidov, A. A.; Lee, S. B.; Aliev, A. E.; Williams, C. D.; Atkinson, K. R.; Baughman, R. H. Strong, Transparent, Multifunctional, Carbon Nanotube Sheets. *Science* **2005**, *309*, 1215–1219.
26. Zahab, A.; Spina, L.; Poncharal, P.; Marlière, C. Water-Vapor Effect on the Electrical Conductivity of a Single-Walled Carbon Nanotube Mat. *Phys. Rev. B* **2000**, *62*, 10000.
27. Valentini, L.; Mercuri, F.; Armentano, I.; Cantalini, C.; Picozzi, S.; Lozzi, L.; Santucci, S.; Sgamellotti, A.; Kenny, J. M. Role of Defects on the Gas Sensing Properties of Carbon Nanotubes Thin Films: Experiment and Theory. *Chem. Phys. Lett.* **2004**, *387*, 356–361.
28. Klinke, C.; Chen, J.; Afzali, A.; Avouris, P. Charge Transfer Induced Polarity Switching in Carbon Nanotube Transistors. *Nano Lett.* **2005**, *5*, 555–558.
29. Dettlaff-Weglikowska, U.; Skakalova, V.; Graupner, R.; Jhang, S. H.; Kim, B. H.; Lee, H. J.; Ley, L.; Park, Y. W.; Berber, S.; Tomanek, D. *et al.* Effect of $SOCl_2$ Treatment on Electrical and Mechanical Properties of Single-Wall Carbon Nanotube Networks. *J. Am. Chem. Soc.* **2005**, *127*, 5125–5131.
30. Miyata, Y.; Yanagi, K.; Maniwa, Y.; Kataura, H. Highly Stabilized Conductivity of Metallic Single Wall Carbon Nanotube Thin Films. *J. Phys. Chem. C* **2008**, *110*, 3591–3596.
31. Bekyarova, E.; Itkis, M. E.; Cabrera, N.; Zhao, B.; Yu, A. P.; Gao, J. B.; Haddon, R. C. Electronic Properties of Single-Walled Carbon Nanotube Networks. *J. Am. Chem. Soc.* **2005**, *127*, 5990–5995.
32. Sheng, P. Fluctuation-Induced Tunneling Conduction in Disordered Materials. *Phys. Rev. B* **1980**, *21*, 2180.
33. Stadermann, M.; Papadakis, S. J.; Falvo, M. R.; Novak, J.; Snow, E.; Fu, Q.; Liu, J.; Fridman, Y.; Boland, J. J.; Superfine, R. *et al.* Nanoscale Study of Conduction through Carbon Nanotube Networks. *Phys. Rev. B* **2004**, *69*, 201402(R)
34. Kong, J.; Franklin, N. R.; Zhou, C.; Chapline, M. G.; Peng, S.; Cho, K.; Dai, H. Nanotube Molecular Wires as Chemical Sensors. *Science* **2000**, *287*, 622–625.
35. Derycke, V.; Martel, R.; Appenzeller, J.; Avouris, P. Controlling Doping and Carrier Injection in Carbon Nanotube Transistors. *Appl. Phys. Lett.* **2002**, *80*, 2773–2775.
36. Yang, C. M.; Park, J. S.; An, K. H.; Lim, S. C.; Seo, K.; Kim, B.; Park, K. A.; Han, S.; Park, C. Y.; Lee, Y. H. Selective Removal of Metallic Single-Walled Carbon Nanotubes with Small Diameters by Using Nitric and Sulfuric Acids. *J. Phys. Chem. B* **2005**, *109*, 19242–19248.
37. Maeda, Y.; Kimura, S. I.; Kanda, M.; Hirashima, Y.; Hasegawa, T.; Wakahara, T.; Lian, Y.; Nakahodo, T.; Tsuchiya, T.; Akasaka, T. *et al.* Large-Scale Separation of Metallic and Semiconducting Single-Walled Carbon Nanotubes. *J. Am. Chem. Soc.* **2005**, *127*, 10287–10290.
38. Linstrom, P. J.; Mallard, W. G. E. *NIST Chemistry Webbook, NIST Standard Reference Database Number 69*; http://webbook.nist.gov (April 2008).